Inorganic Materials, Vol. 37, No. 10, 2001, pp. 1037–1040. Translated from Neorganicheskie Materialy, Vol. 37, No. 10, 2001, pp. 1219–1223.

Hollow Alumina Macrotubes

S. S. Berdonosov, S. B. Baronov, Yu. V. Kuz'micheva, D. G. Berdonosova, and I. V. Melikhov

Moscow State University, Moscow, 119899 Russia

e-mail: melikhov@radio.chem.msu.ru

Received February 28, 2001; in final form, April 18, 2001

Abstract—Poorly crystallized Al_2O_3 macrotubes 50 μm to 6 cm in length, 10 to 300 μm in outer diameter, and 2 to 60 μm in inner diameter were obtained by heating partially hydrolyzed $AlCl_3$ powder to 170–220°C in a flowing inert gas or air. The tubes were characterized by electron microscopy, atomic-force microscopy, IR spectroscopy, x-ray diffraction, and electron probe microanalysis.

INTRODUCTION

Recent findings in fullerene research have sparked wide interest in the preparation of fullerene-like carbon tubes [1–4]. Not only nano- and microtubes but also macroscopic carbon tubes up to several centimeters in length could be produced [5]. It is reasonable to expect that macrotubes can also be produced by chemical means from other materials.

This was confirmed in our experiments by growing alumina tubes up to 6 cm in length, 10–300 μm in outer diameter, and 2–60 μm in inner diameter.

TUBE GROWTH

The starting material was anhydrous $AlCl_3$ prepared by chlorinating high-purity metallic aluminum (as found later, the purity of Al had no effect on the formation of macrotubes) and purified by sublimation in an evacuated ampule to remove nonvolatile contaminants. $AlCl_3$ (0.5 g) was placed in a porcelain boat and exposed for 0.25–48 h to humid air (water vapor pressure of ≃2.7 kPa). Next, the boat with the partially hydrolyzed product was transferred to a quartz tube ≤4 cm in diameter, fitted with a heating coil.

Hydrated aluminum chloride is known to be nonvolatile, unlike anhydrous $AlCl_3$, and to decompose above 150–250°C to form hydrogen chloride, $AlCl_3$ vapor, and Al_2O_3.

In our experiments, heating the partially hydrolyzed $AlCl_3$ powder to 100–150°C gave rise to random motion of powder particles, some of which even escaped the boat. This was presumably caused by nonuniform decomposition of the hydroxychlorides produced by $AlCl_3$ hydrolysis. At this stage, a rough crust was formed on the sample surface.

Starting at 150°C, small hillocks and then openings appeared on the crust surface. Some of the openings exhaled jets of white steam. At 180°C, short transparent tubes perpendicular or inclined to the sample surface became visible (Fig. 1). The tubes continued to exhale steam and grew rapidly (≃1 mm/s) in length.

Steaming became weaker as the tubes grew longer. Occasionally, it ceased for several seconds and then resumed. The tube then continued to grow, but its diameter decreased abruptly (Fig. 2).

When steam exhalation was over, the tube growth stopped. At a heating rate of 60°C/min, the formation of tubes took, on average, 30 s.

After the tubes stopped growing, the heater was switched off, and the boat was taken out of the reactor. From one to a hundred tubes grew in a run. The largest length of the tubes was 6 cm, and their average weight was 20 μg.

CHARACTERIZATION OF MACROTUBES

The macrotubes possessed a relatively high elasticity: the thinnest tubes, ranging up to 2–2.5 cm in length, did not break when bent through 120°–180°.

Under an optical microscope, the tubes were seen to consist of transparent material. Their lustrous surface was covered with a white deposit, which could be removed mechanically (for instance, with a spatula).

The tubes were examined by optical microscopy (MZ12 Leica microscope, Quantimet 550IW image

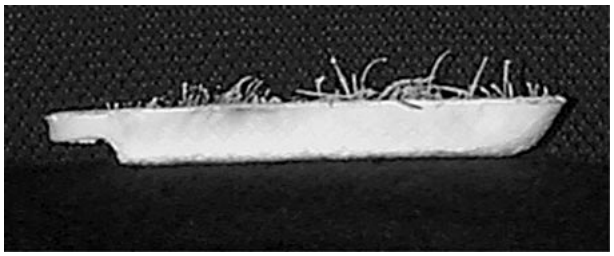

Fig. 1. Boat with tubular alumina fibers.

0020-1685/01/3710-1037$25.00 © 2001 MAIK "Nauka/Interperiodica"

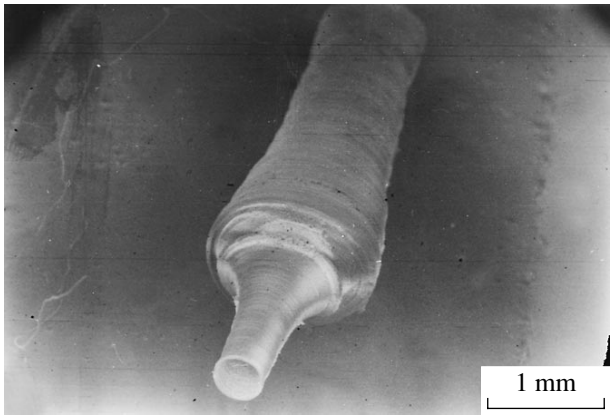

Fig. 2. Macrotube with a varying outer diameter.

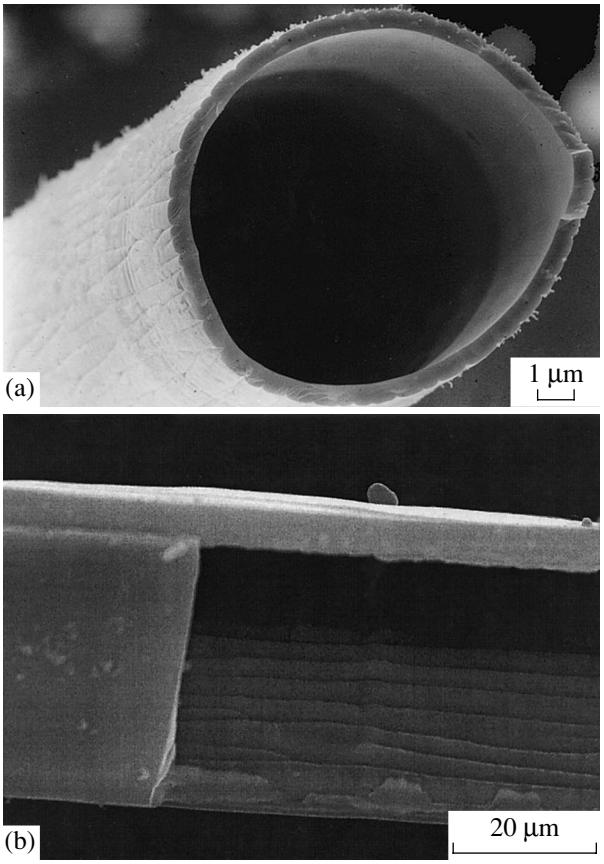

Fig. 3. SEM micrographs illustrating the (a) external and (b) internal morphology of macrotubes.

analysis system), scanning electron microscopy (SEM) (JEOL and Amray instruments), electron microprobe analysis (ISIS Oxford Instruments microanalyzer operated at 20 kV), atomic-force microscopy (AFM) (P47-SPM-MDT Solver instrument), and IR spectroscopy (Spectrum-2000 Perkin-Elmer Fourier-transform IR spectrophotometer equipped with an IR microscope and liquid-nitrogen-cooled HgCdTe detector). The tube material was also characterized by x-ray diffraction (Debye–Scherrer and Laue photographs) and selected-area diffraction (SAD) on a JEM-100B electron microscope.

The tubes were found to have rather smooth inner and outer surfaces (Fig. 3), typically with a beaded or bell-mouthed free end (Fig. 4) and without encapsulated material. Each tube was, most likely, made up of several fragments.

According to microprobe analysis data, the tubes consisted of oxygen, aluminum, and trace amounts of chlorine (table). If a small amount (≤5 mol %) of $FeCl_3$ was added to $AlCl_3$, and the hydrolyzed material was heated in a hydrogen atmosphere, the resulting α-Fe (identified by x-ray diffraction) was concentrated mainly at the free tube end (table).

Similar tubes grew if ≤40 mol % NH_4Cl was added to $AlCl_3$. Attempts to produce macrotubes via partial hydrolysis of anhydrous $FeCl_3$ or $ZrCl_4$, followed by heat treatment, were unsuccessful.

AFM examination showed that the outer surface layer consisted of irregularly shaped particles, arranged with no periodicity (Fig. 5a).

The inner surface was formed by tightly packed elongated cylindrical particles up to 2.5 μm in radius (Fig. 5b), occasionally with bumps ≃250 nm across (Fig. 5c), or it was smooth, with height variations within 10–15 nm over a 20-μm^2 area (Fig. 5d). The smooth surface was typical of the lower part of the tubes, and the wavy surface was typical of the upper part, with a sharp transition from one surface morphology to the other.

The x-ray pattern (CuK_α radiation) from ground tubes (Fig. 6) showed three weak peaks (2θ = 43.7°, 51.2°, and 56.66°) attributable to corundum. From SAD patterns, the phase composition of the tubes could not be determined.

Comparison of the IR spectrum of the tubes (Fig. 7) with earlier data [6] led us to conclude that the tubes consisted of Al_2O_3.

GROWTH MECHANISM

Based on the present results, Al_2O_3 macrotubes seem to grow by the following mechanism: After exposure to water vapor, the hydrolyzed surface layer of $AlCl_3$ particles contains OH groups and water molecules. During subsequent heating, the hydrolysis products decompose, and water rapidly vaporizes from the top layer of the sample. The resulting gas-tight crust consists of Al_2O_3 and aluminum hydroxychlorides. The underlayer consists of undecomposed aluminum hydroxychlorides and unreacted $AlCl_3$. Further heating gives rise to the decomposition of the hydroxychlorides and $AlCl_3$ hydrolysis under the crust, leading to the formation of water vapor and hydrogen chloride. In addition, the $AlCl_3$ vapor pressure becomes noticeable at 150–160°C and increases rapidly at higher temperatures.

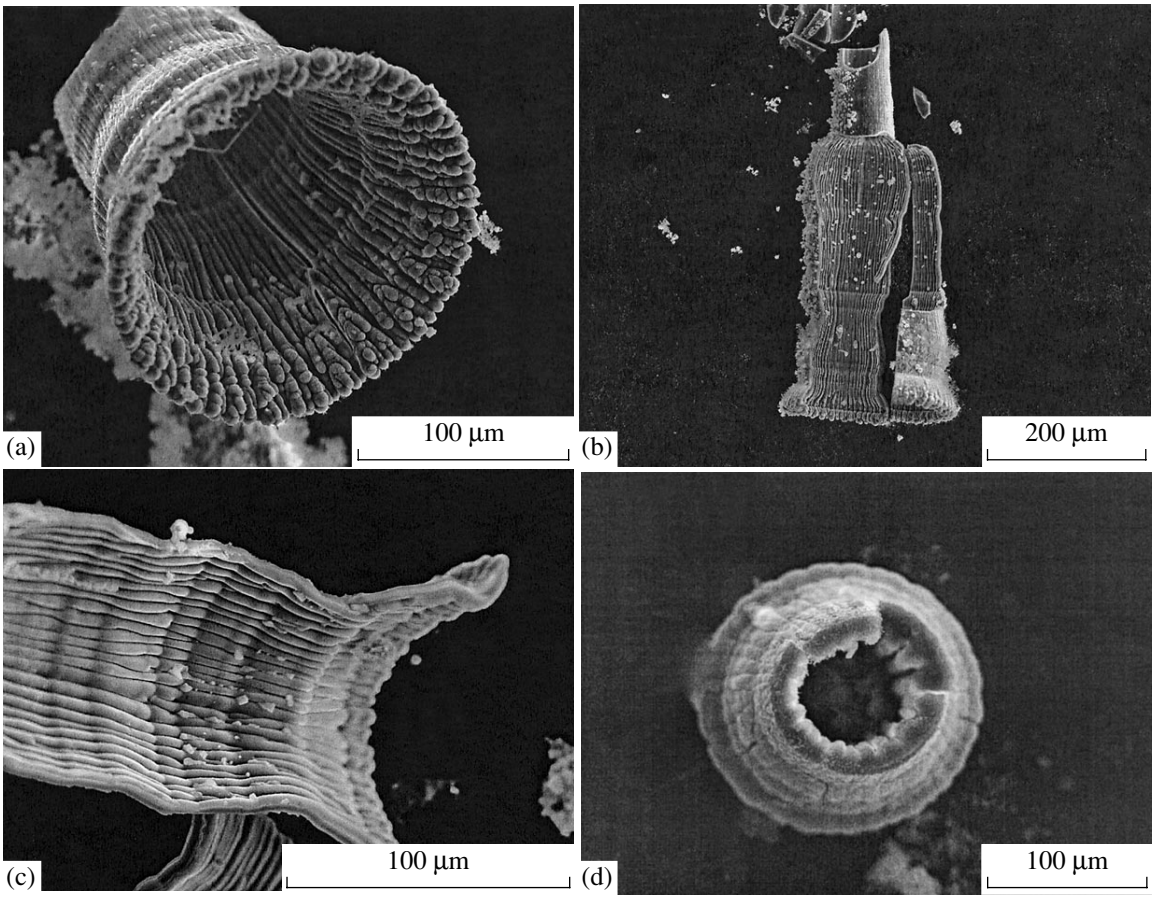

Fig. 4. SEM micrographs of typical (a–c) beaded and (d) bell-mouthed macrotubes: (a, b, d) external view, (c) inner surface.

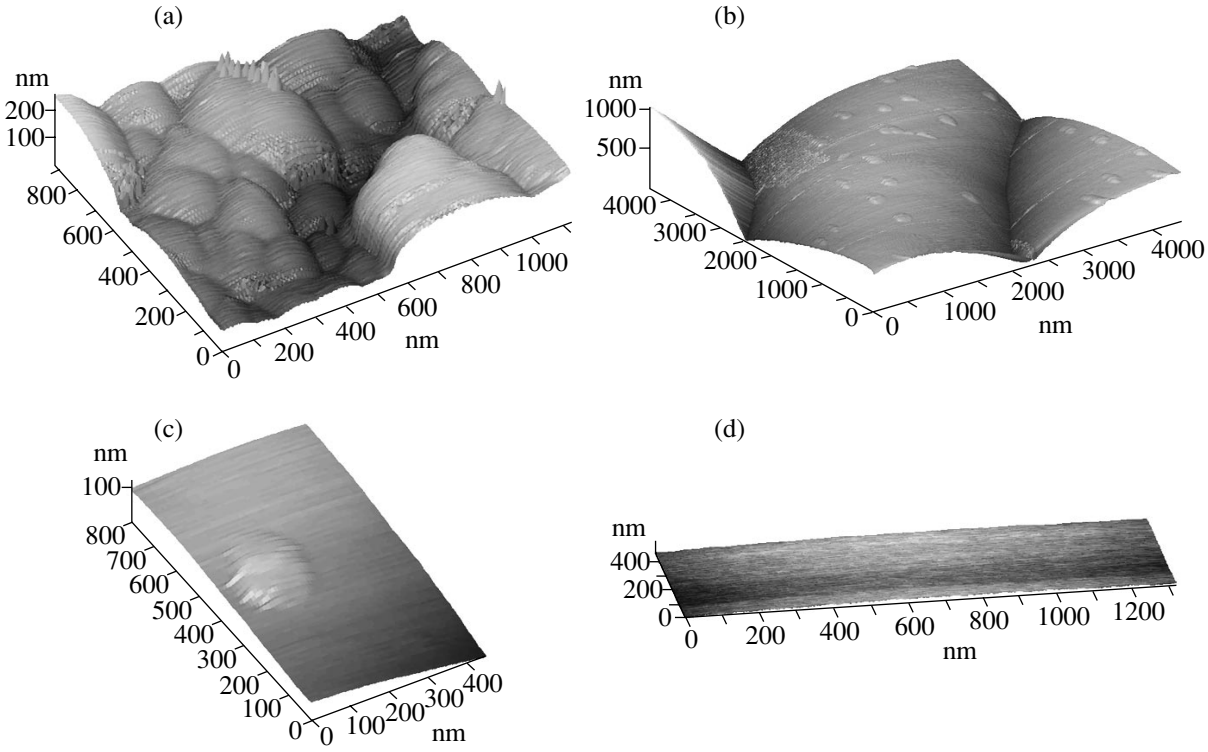

Fig. 5. AFM topographic images of the (a) outer and (b–d) inner surfaces of macrotubes.

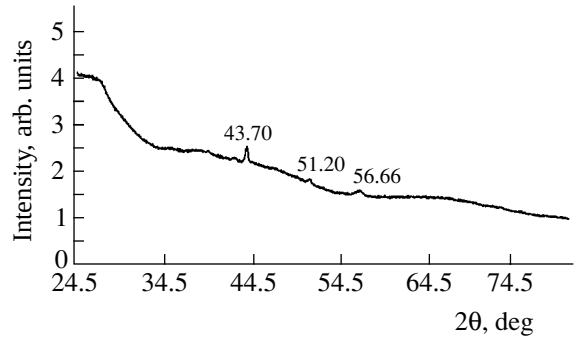

Fig. 6. X-ray pattern of ground macrotubes.

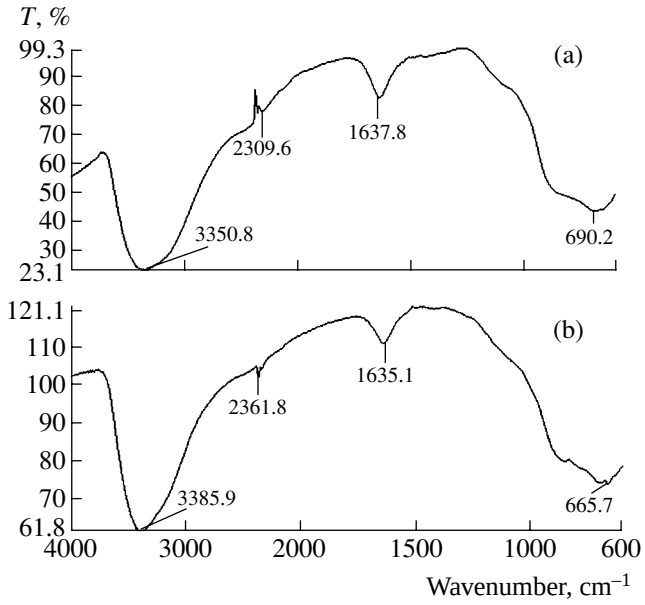

Fig. 7. IR spectra of (a) macrotubes and (b) Al_2O_3 [6].

As a result of the rise in internal pressure, the vapor breaks through the crust, producing a "microvolcano" on the sample surface, with the elevated crater edge consisting of Al_2O_3.

The release of water, $AlCl_3$, and HCl vapors is accompanied by further formation of Al_2O_3, which is nonvolatile under the conditions of this study. As a result, aggregates of Al_2O_3 particles less than 1 μm in size are formed in the vapor phase (such particles constitute the white deposit forming on the wall of the quartz reactor). Since the submicron particles have a high surface energy, they readily become attached to the crater edge, feeding the further growth of the macrotube.

As a result, the tube grows rapidly in length, whereas its outer diameter remains unchanged. Since the exhalation of $AlCl_3$ vapor from the sample is unsteady, the tubes consist of microscopic regions differing in dimensions. If part of a tube breaks off accidentally, subsequent growth is often accompanied by a reduction in tube diameter (Fig. 2).

If the starting charge contains $FeCl_3$, the dopant vaporizes in the final stage of heat treatment, because the vapor pressure of $FeCl_3$ is much lower than that of $AlCl_3$. If the process is run in hydrogen and the temperature is high enough for rapid reduction of $FeCl_3$, we find metallic iron at the free tube end.

Al_2O_3 tubes grown by the method described above are potentially attractive as catalyst supports and substrates for conducting films. This method is probably also applicable for producing macrotubes of other oxides.

Microanalysis data for macrotubes grown from $AlCl_3$ (I) and 95 mol % $AlCl_3$ + 5 mol % $FeCl_3$ (II)

Element	Weight percent	
	I	II
Al	32–42	17–26
O	44–60	22–30
Cl	3–7	1–3
Fe	–	32–75

CONCLUSION

Poorly crystallized alumina macrotubes 50 μm to 6 cm in length, 10 to 300 μm in outer diameter, and 2 to 60 μm in inner diameter were produced by thermal decomposition of partially hydrolyzed $AlCl_3$ in a gaseous atmosphere.

ACKNOWLEDGMENTS

We thank E.V. Antipov, A.V. Bogdanov, A.G. Bogdanov, I.A. Budashov, Yu.A. Velikodnyi, I.N. Kurochkin, F.M. Spiridonov, and M.A. Prokof'ev for their assistance with this study and useful discussions and N.N. Oleinikov for valuable suggestions.

This work was supported by the Russian Foundation for Basic Research, grants no. 99-03-32646 and no. 00-03-32644.

REFERENCES

1. Ting, J.-M. and Lan, J.B.C., Beaded Carbon Tubes, *Appl. Phys. Lett.*, 1999, vol. 75, no. 21, pp. 3309–3311.
2. Dagani, R., Much Ado about Nanotubes, *Chem. Eng. News*, 1999, vol. 77, no. 2, pp. 31–34.
3. Rakov, E.G., Preparation of Carbon Nanotubes, *Usp. Khim.*, 2000, vol. 69, no. 1, pp. 41–59.
4. Ma, X., Wang, E., Zhou, W., *et al.*, Polymerized Carbon Nanobells and Their Field-Emission Properties, *Appl. Phys. Lett.*, 1999, vol. 75, no. 20, pp. 3105–3107.
5. Ajayan, P.M., Nugent, J.M., Siegel, R.W., *et al.*, Growth of Carbon Micro-Trees, *Nature* (London), 2000, vol. 404, no. 6775, p. 243.
6. Hummel, D.O. and Schol, F., *Atlas of Polymer and Plastics Analysis*, Vienna: Henzer, 1982, vol. 2, part A, II, p. 891, Spektrum 4444.